Int. J. Electrochem. Sci., 3 **(2008)** 891 - 907

International Journal of ELECTROCHEMICAL SCIENCE
www.electrochemsci.org

Studies on the Effect of B and B+Ce Additions on the Electrochemical Corrosion Behaviour of 9Cr-1Mo Using Electrochemical Noise (EN) Technique

M. G. Pujar[1], *K. Laha*[1], *R. K. Dayal*[1] *and N. Shinya*[2]

[1] Metallurgy and Materials Group (MMG), Indira Gandhi Centre for Atomic Research (IGCAR) Kalpakkam – 603 102, Tamil Nadu, India
[2] National Institute for Materials Science (NIMS), Japan
*E-mail: pujar55@gmail.com

Received: 16 May 2008 / *Accepted:* 3 June / *Online Published:* 30 June 2008

Though strategically important, ferritic steels like 9Cr-1Mo undergo high corrosion in acidic and chloride containing environments. Additions of metalloids and rare earth metals in minute quantities are being attempted to arrest corrosion and improve their properties. In the present paper, general corrosion behaviour of 9Cr-1Mo with and without the additions of B, B+Ce (< 100 ppm) has been studied in deaerated sulphuric acid using electrochemical noise (EN) technique. Visual records of the current and the potential signals along with the extensive statistical analysis of the correlated current and potential data as well as the spectral estimation to study the power in the current signals revealed that addition of B and B+Ce was beneficial in improving uniform corrosion resistance of 9Cr-1Mo significantly. Addition of B resulted in somewhat superior corrosion resistance compared to the B+Ce addition. Boron addition also lent good passivability to 9Cr-1Mo compared to B+Ce addition.

Keywords: 9Cr-1Mo; Boron; Cerium; Electrochemical Noise, Corrosion

1. INTRODUCTION

Ferritic steels like 9Cr-1Mo are of great strategic importance in the fast reactor programme, as they are widely used as the construction materials for the steam generators and safety grade decay heat system. 9Cr-1Mo ferritic steel is one of the high temperature materials extensively used in the chemical, petroleum and power generating industries because of its improved mechanical and corrosion resistance properties [1-3]. This is because of the fact that properly heat-treated 9Cr-1Mo is regarded as having good resistance to stress corrosion cracking (SCC) in both acidic chlorides [4] and alkaline solution under freely corroding conditions [4, 5]. Though, 9Cr-1Mo steels have good SCC

resistance in acidic chloride and alkalies, they are subject to high rates of corrosion in non-oxidising conditions of sulphuric acid and hydrochloric acid solutions [6]. It is reported that addition of metalloids like boron, phosphorus and silicon to amorphous Fe-Cr alloys resulted in considerable improvement in the general and the localised corrosion resistance. It was found that the homogeneity of the alloys was independent of the composition of the amorphous alloys, and hence was unaffected by the change in the metalloid addition. These amorphous alloys exhibited good corrosion resistance owing to the formation of a homogeneous, stable and defectless passive film [7]. Recently it was reported by Mottat et al. [8] that chromium-metalloid materials resembled that of chromium-noble-metal alloys and that alloying with phosphorus and boron promoted spontaneous passivation of chromium in reducing acids. Thus, it was reasoned that in terms of economic considerations, one could use metalloids rather than platinum-group metals (PGM) as alloying elements to increase the corrosion resistance of Fe-Cr alloys [6]. Apart from the metalloids, it is well known that the addition of rare earth elements (REM) showed improvement in corrosion resistance of various materials, regardless of the aggressive environment [9]. Among the rare earth elements, cerium is found to be of great importance. Significant improvement in corrosion resistance of various alloys in different aggressive environments was achieved by adding cerium in small concentrations [10-13]. In the present paper, an attempt is made to study the effect of the addition of B and B+Ce (<100 ppm) on the uniform corrosion behaviour of 9Cr-1Mo steel; the investigations were conducted using EN technique. The conventional term "passive film" is used in the paper for convenience although it is already established [14] that the film formed on these steels in an acidic medium is composed of the loose corrosion deposits and is unstable.

2. EXPERIMENTAL PART

9Cr-1Mo specimens with additions of Boron and Boron+Cerium were used in the present study. The chemical composition of the specimens is given in Table 1. The electrochemical noise studies on this material were performed using two nominally identical cylindrical electrodes of the same size (10 mm diameter and 25 mm length) that were polished up to fine diamond (1μm finish), washed in soap water and degreased in acetone. While immersing the electrodes in the solution care was taken to expose minimum lateral surface area to the solution; rest of the electrode was covered completely with Teflon tape. The area of the electrode surface immersed in the solution was about 0.8 cm^2. Potential and current noise measurements were performed by shorting together two identical working electrodes. The current flowing between the two working electrodes, as well as the potential between the working electrode and a reference electrode were monitored. Electrochemical current and potential noise studies were conducted in deaerated 0.5M sulphuric acid at open circuit potential (OCP) and the signals were collected at the sampling frequency of 4 Hz. Saturated calomel electrode (SCE) was used as the reference electrode for the measurement of potential noise.

The potentiostat, which can perform this experiment actively, holds the working electrode connection at the 'ground' potential by a small amplifier circuit. If one 'working' electrode is directly connected to ground and the other is connected to the working electrode cable, they are both held at the

same potential and are, in effect, 'shorted' together. Any current, which flows between the two electrodes, is measured by the instruments of current measurement circuits thus creating a Zero Resistance Ammeter (ZRA). The potential is measured between the 'working' electrodes (since they are shorted together, both 'working' electrodes are at the same potential) and a reference electrode.

Table 1. Chemical composition (wt.%) of the steels

Steels	C	Mn	P	S	Si	Cr	Mo	V	Nb	N	Al	Ni	B	Ce
9Cr-1Mo	0.110	0.34	0.021	0.0021	0.31	9.04	0.98	0.23	0.069	0.051	0.009	0.09	-	-
9Cr-1Mo with B	0.110	0.33	0.023	0.0019	0.34	9.03	1.02	0.20	0.068	0.049	0.089	0.10	0.011	-
9Cr-1Mo with B+Ce	0.110	0.31	0.020	0.0018	0.37	9.01	0.99	0.21	0.07	0.054	0.011	0.99	0.009	0.069

The linear trend component was estimated by least squares method and then eliminated by subtraction using commercial software from the acquired data. A set of 1024 data points was analysed to calculate statistical parameters as well as PSD plots. All the potential and current noise data collected in the time domain were transformed in the frequency domain through the Maximum Entropy Method (MEM) method, by a dedicated software. It has been reported that the MEM computed with few coefficients (known as M) produces a very smooth spectrum, preferable to that obtained by Fast Fourier Transform (FFT), even after averaging and that is why low values of M are commonly used in corrosion applications [15]. Bertocci et al. [16] reported that MEM computed with an order of 10 gave better precision than FFT with one average and lower values of M were adequate. Thus, in the present work, Power Spectral Density (PSD) data were obtained by computing MEM with an order of 15. In order to reduce the leakage of the low as well as the high frequencies in the calculated PSD values, Welch window was used for signal analysis.

Potentiodynamic anodic polarisation studies were conducted using a three-electrode assembly consisting of a working electrode (material under study), counter electrode (two platinum electrodes shorted together) and a reference electrode (SCE) in deaerated 0.5M sulphuric acid. The solution was deaerated to remove oxygen by bubbling oxygen-free and moisture-free argon gas through the solution for one hour before the specimen was immersed; bubbling argon was continued till the experiment was completed. On immersion of the specimen, a 30 min time interval was allowed for attaining stable OCP. Thereafter, anodic polarisation experiment was conducted through a potential range from –1.0 V to 1.5 V(SCE) at the scan rate of 10 mV/min.

In order to calculate corrosion rates using Three Point Method (TPM) as well as Four Point Method (FPM) potentiodynamic anodic polarization experiments were conducted in a limited potential range. After immersion of the specimen, 30 min time was allowed for the stabilization of the OCP. Potentiodynamic anodic polarization experiments were conducted in a potential range of –0.1V(OCP) to +0.1V(OCP), the potentials being measured against SCE. The polarization experiments were

conducted at 10 mV/min scan rates. Corrosion rates were calculated according to two methods (Method 1 and Method 2) under TPM as suggested by Danielson [17] as well as using FPM as given by Jankowski [18]. The corrosion rates were also obtained using Tafel fitting technique to obtain Tafel slopes as well as corrosion rates.

3. RESULTS AND DISCUSSION

Figure 1(a-c) shows the optical photomicrographs of the three alloys which were obtained after the normalizing and tempering treatment. It was observed that all the three alloys showed tempered martensite laths and there were carbides decorating the boundaries of these laths. The microstructure also shows the prior austenite grain boundaries. There was no distinction in the microstructures on account of the addition of Boron or Boron and Cerium. The visual records of current and potential signals for all the specimens are presented in Fig. 2 (a, b). It was observed that 9Cr-1Mo without any addition and with the addition of B+Ce showed consistently anodic current transients, whereas 9Cr-1Mo with the addition of B showed current transients that were in cathodic region. 9Cr-1Mo showed an initial decrease in the anodic current, which started to increase at about 1000s, and reached a saturation value at about 3000s; thereafter the variation in the current was insignificant. Although 9Cr-1Mo with B+Ce showed consistently anodic current signals, the anodic current was less than that exhibited by 9Cr-1Mo. 9Cr-1Mo with addition of B showed a continuously decreasing trend of cathodic current indicating a stable passive film formation which did not dissolve till the end of the experiment. The potential signal plot was marked by the characteristic noble potential signal shown by 9Cr-1Mo with the addition of B, which exhibited noble potentials in a range – 0.41 V to – 0.38 V (SCE) for about initial 6000s that later stabilised at about – 0.45 V (SCE). The potentials signals exhibited by 9Cr-1Mo with and without the addition of B+Ce were active compared to the ones exhibited by B added specimen. The specimen with B+Ce addition showed a brief initial rise of the potential in the anodic direction for about 3000s but dropped to a constant lower value of about – 0.48 V (SCE) and remained unchanged thereafter. The specimen without any addition showed the most active potentials throughout, signifying its least corrosion resistance among the three alloys studied.

The statistical parameters like standard deviation of current, σ_I, standard deviation of potential, σ_V, mean current, mean potential were calculated at an interval of 2500s for convenience from the detrended data. The σ_I and σ_V values basically indicate the current and potential amplitude respectively. It was observed (Fig. 3a) that the σ_I values were highest for the 9Cr-1Mo specimen compared to other two specimens, which apparently would mean higher corrosion rate of the former specimen. The specimens with the additions of B and B+Ce respectively showed the lower σ_I values which decreased continuously with time. At the end of the 12500s, the specimen with B addition showed the lowest σ_I value which indicated that it had better corrosion resistance compared to the other two specimens. The σ_V values (Fig. 3b) showed somewhat different trends. The specimen with B addition showed higher values of σ_V compared to the specimens with and without the addition of B+Ce, which showed decreasing trend of the σ_V values.

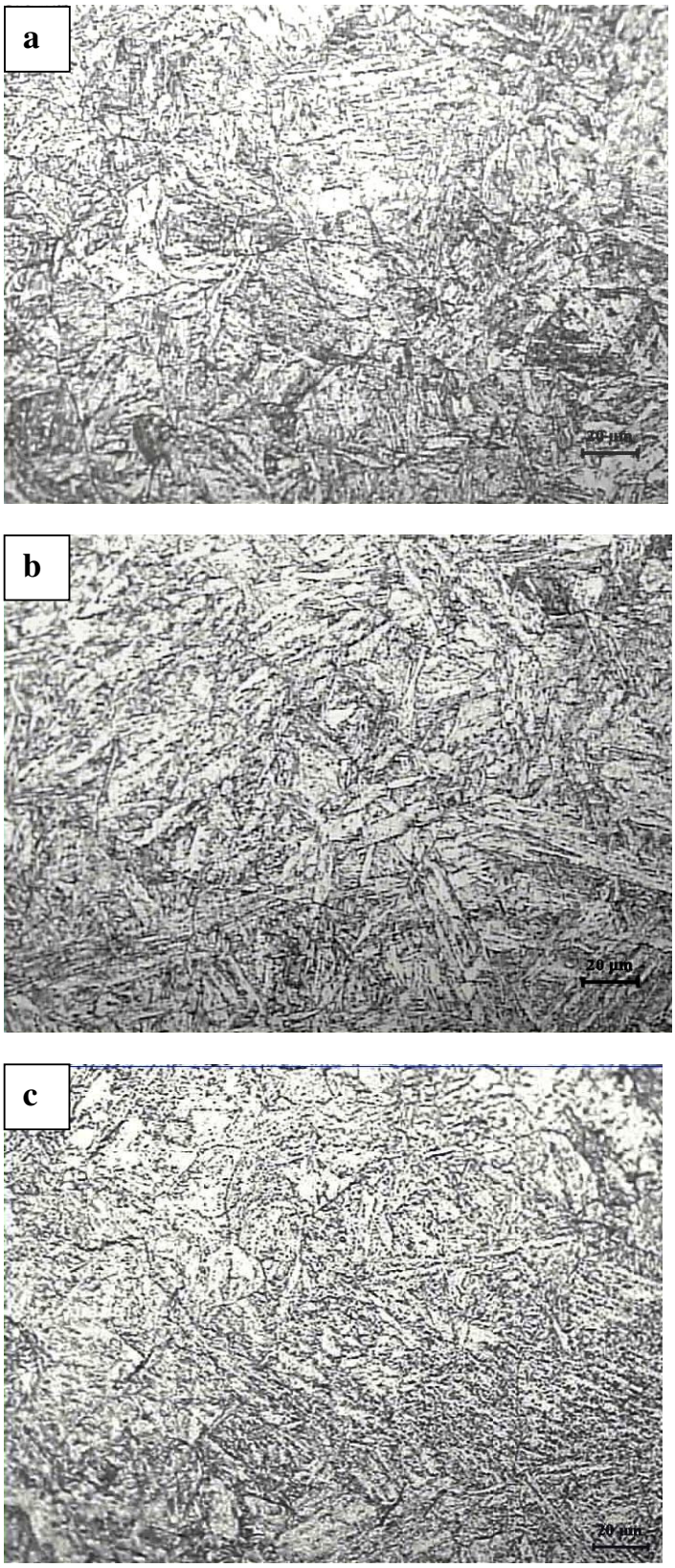

Figure 1. Photomicrographs showing the microstructure of (a) 9Cr-1Mo Plain, (b) 9Cr-1Mo with B addition and (c) and 9Cr-1Mo with B+Ce addition

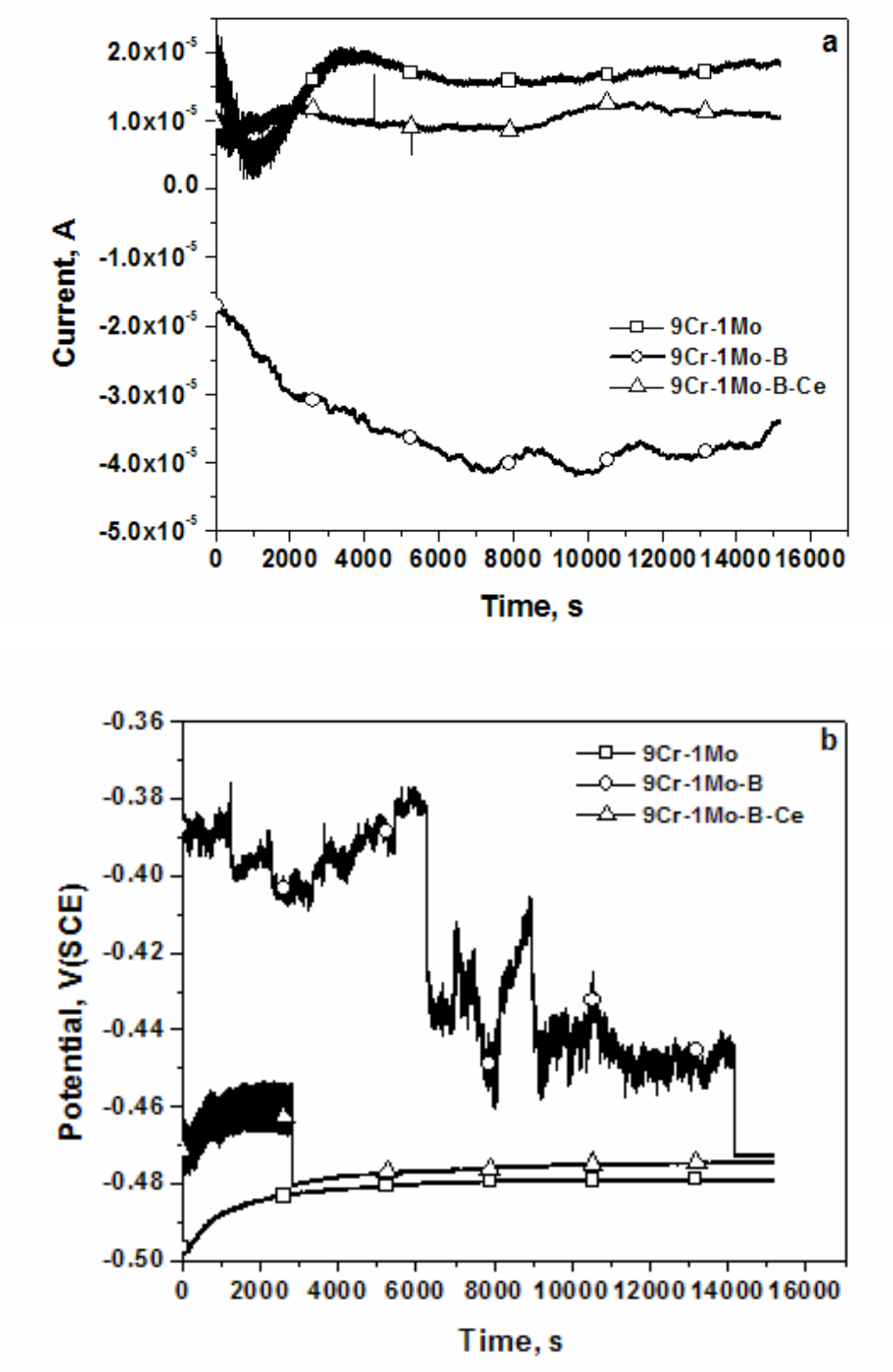

Figure 2. Records of electrochemical current (a) and potential (b) signals for 9Cr-1Mo steel with the additions of B and B+Ce in deaerated sulphuric acid.

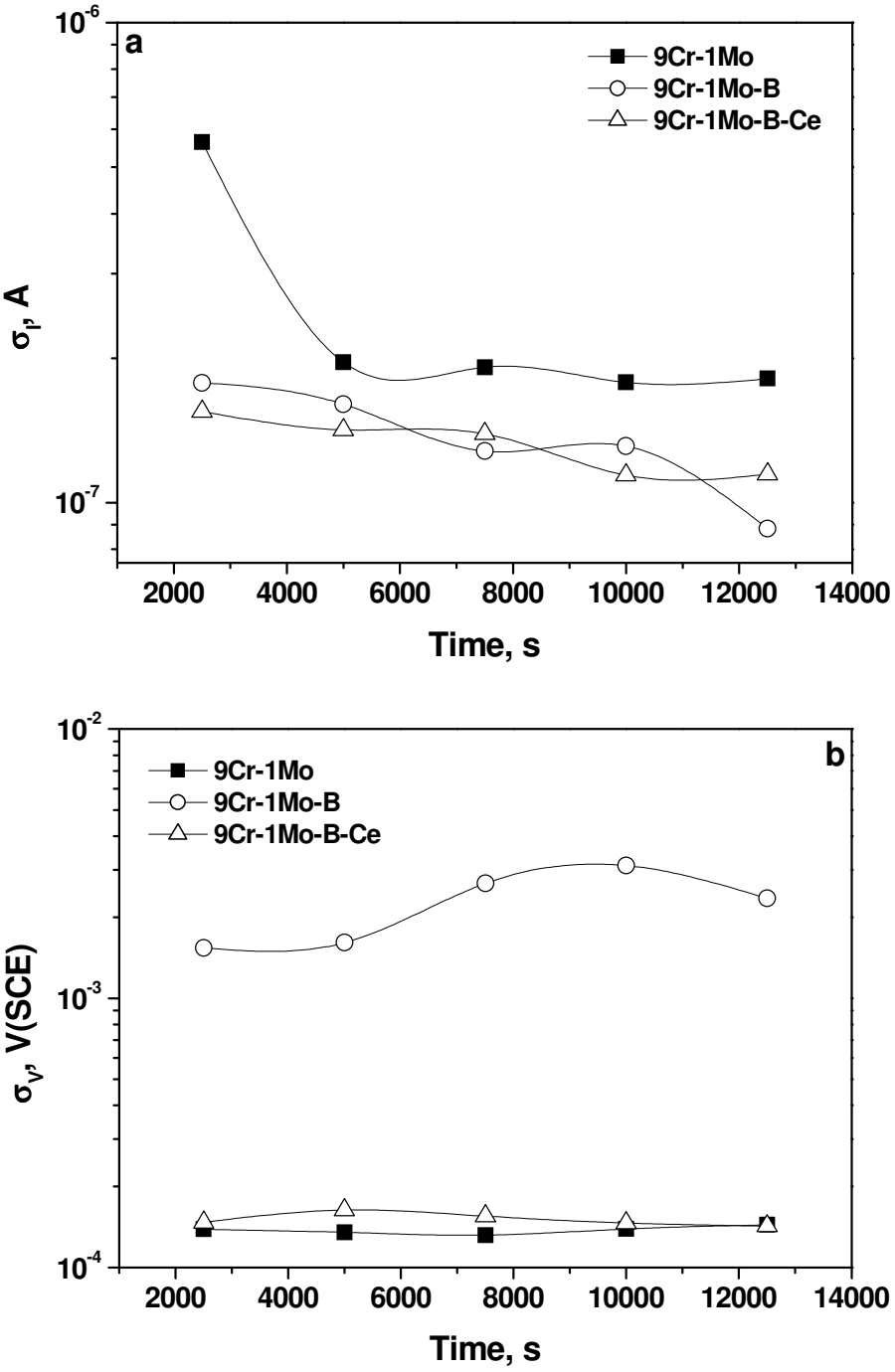

Figure 3. Standard deviation of current, σ_I (a) and standard deviation of potential, σ_V (b) for 9Cr-1Mo with additions of B and B+Ce in deaerated sulphuric acid.

Mean current and mean potential values are not considered to be the true statistical parameters and thus these values were obtained from the raw data and are shown in Fig. 4 (a, b). It was observed that the mean current values shown by the specimen with and without the addition of B+Ce were much higher and anodic in nature as compared to the values shown by the specimen with B addition. The specimen without any addition showed the highest values of the mean current indicating a constant dissolution of the passive film at a higher rate. The specimen with B addition showed mean current values that were cathodic in nature and which decreased gradually to a stable value at about 8000s. This observation reinforces the fact that the passive film on the surface of the specimen with B addition was much more stable and did not dissolve easily whereas the passive film formed over other specimens gradually dissolved leading to anodic currents. The specimen with the addition of B initially showed an initial decrease in the mean potentials values which reached an almost stable value of about – 0.44V to – 0.45 V(SCE). The B added specimen nevertheless showed more noble mean potential values compared to the other two specimens. The specimen without any addition showed the most active mean potential values indicating its tendency towards anodic dissolution or undergoing corrosion.

Table 2. The details about various methods given under TPM to calculate corrosion current [13].

Method Adopted	Currents at applied polarisations	Current ratios used	Corrosion current, I_{corr}
Method 1	$I_{\Delta E}$, $I_{2\Delta E}$, $I_{-\Delta E}$	$r_1 = \frac{I_{2\Delta E}}{I_{\Delta E}}$, $r_2 = \frac{I_{\Delta E}}{I_{-\Delta E}}$	$I_{corr} = \frac{I_{\Delta E}}{\left(r_1^2 + 4r_2\right)^{1/2}}$
Method 2	$I_{\Delta E}$, $I_{-\Delta E}$, $I_{-2\Delta E}$	$r_1 = \frac{I_{\Delta E}}{I_{-\Delta E}}$, $r_2 = \frac{I_{-2\Delta E}}{I_{-\Delta E}}$	$I_{corr} = \frac{I_{\Delta E}}{\left[\left(r_1 r_r\right)^2 + 4r_1\right]^{1/2}}$
Method 3	$I_{-\Delta E}$, $I_{-2\Delta E}$, $I_{-3\Delta E}$	$r_1 = \frac{I_{-2\Delta E}}{I_{-\Delta E}}$, $r_2 = \frac{I_{-3\Delta E}}{I_{-\Delta E}}$	$I_{corr} = \frac{-I_{-\Delta E}}{\left(4r_2 - 3r_1^2\right)^{1/2}}$
Method 4	$I_{\Delta E}$, $I_{2\Delta E}$, $I_{3\Delta E}$	$r_1 = \frac{I_{2\Delta E}}{I_{\Delta E}}$, $r_2 = \frac{I_{3\Delta E}}{I_{\Delta E}}$	$I_{corr} = \frac{I_{\Delta E}}{\sqrt{4r_2 - 3r_1^2}}$

Figure 5 shows the potentiodynamic anodic polarisation curves for the specimens obtained in deaerated sulphuric acid. The typical anodic polarisation curves of 9Cr-1Mo in deaerated 0.5M sulphuric acid showed two anodic peaks [19-21]. In the present studies too, two anodic peaks were observed for each specimen, however, there was a sudden slump in the passive current density values in a potential range of 0.5V to 1 V(SCE), which was prominently observed for the specimen without any addition. The specimen without any addition showed the highest critical current density (I_{crit}) value compared to the others specimens. The transpassive potential values were the same for all the specimens. The specimen with the addition of B+Ce showed the least I_{crit} value among the three steels.

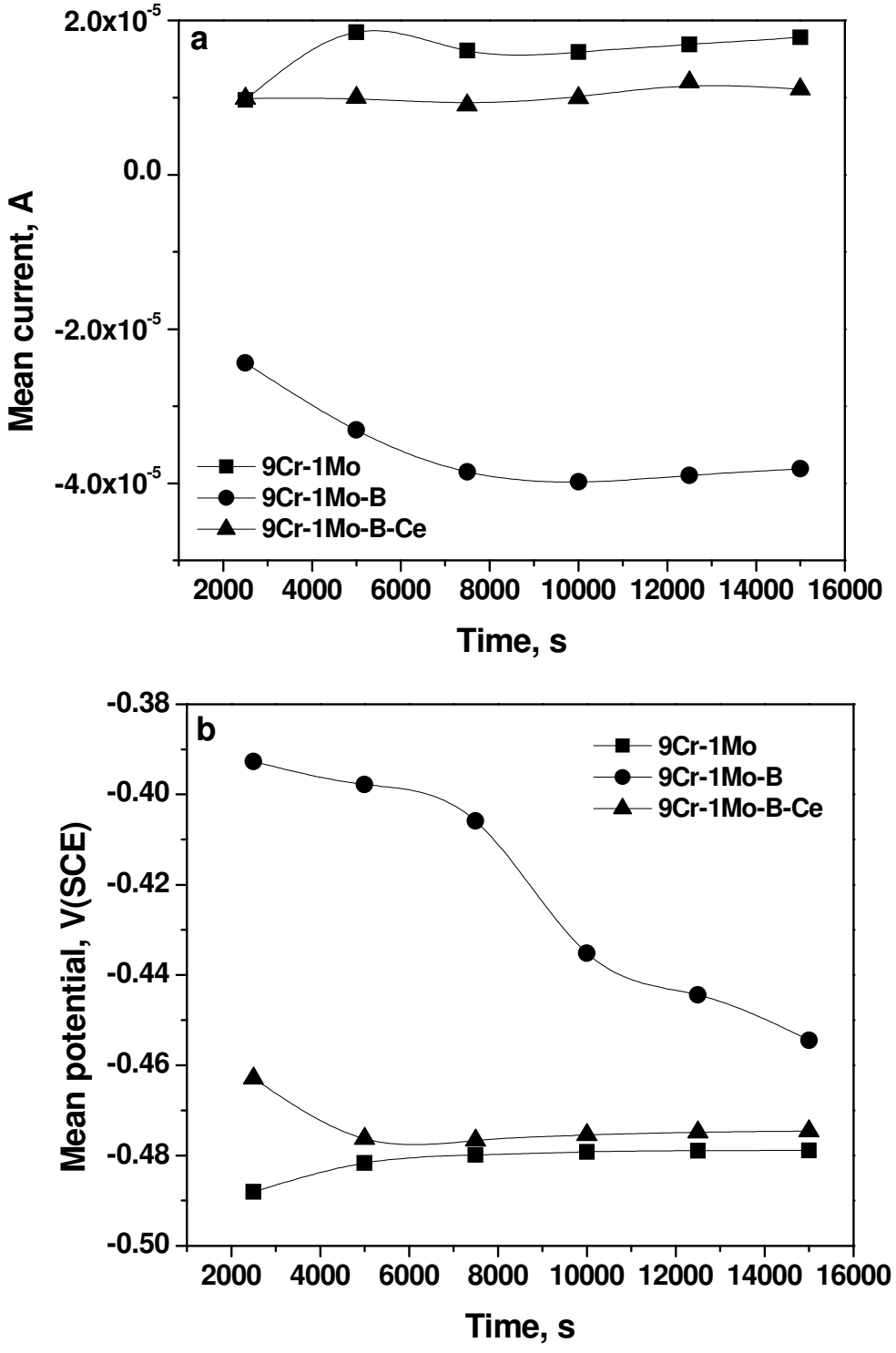

Figure 4. Mean current (a) and mean potential (b) plots for 9Cr-1Mo with additions of B and B+Ce in deaerated sulphuric acid

The following equation given by Wagner and Traud [22], which describes the polarization curve, forms the basis of the TPM as well as FPM and is given below.

$$I = I_{corr}\left\{\exp\frac{2.3\Delta E}{\beta_a} - \exp\frac{-2.3\Delta E}{\beta_c}\right\} \quad \text{----------1)}$$

In the above equation, I is the current at the applied potential E, $\Delta E = E - E_{corr}$, I_{corr} is the corrosion current at the corrosion potential, E_{corr}, β_a and β_c are the Tafel slopes. Barnartt [23] who introduced the TPM for the first time showed that if three different perturbing potentials have a certain relationship to each other, their measured currents could be used to solve the above equation (1) in closed form. Different combinations of potentials and their corresponding currents can be used to arrive at the I_{corr} value. Danielson [17] discussed different combinations of currents corresponding to different potential intervals and suggested four methods under TPM (Table 2). Method 1 uses currents at applied polarizations ΔE, 2ΔE, −ΔE, whereas Method 2 uses currents at applied polarizations ΔE, −ΔE, −2ΔE respectively.

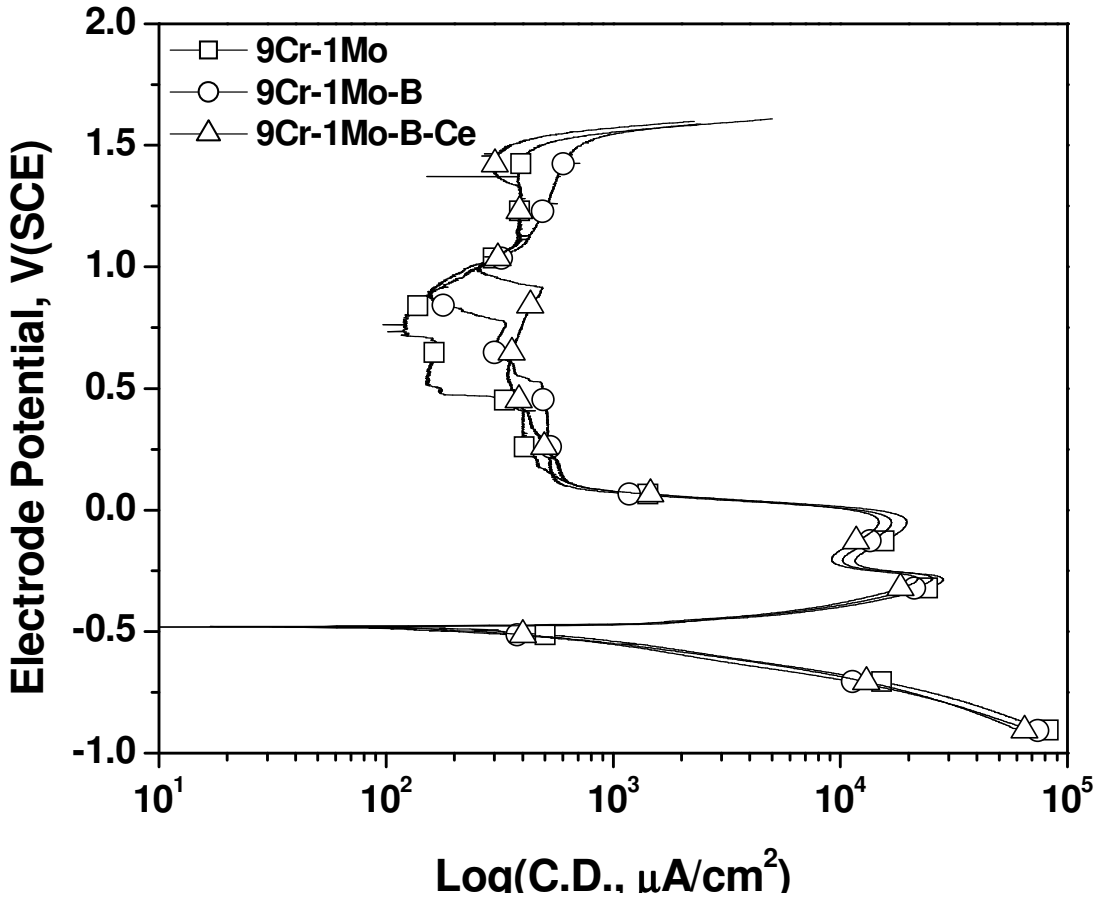

Figure 5. Potentiodynamic anodic polarisation curves for 9Cr-1Mo with additions of B and B+Ce in deaerated 0.5M sulphuric acid solution

Using the above equation (1) and currents at applied polarizations I_1 at ΔE, I_2 at 2ΔE (anodic polarization), I_{-1} at –ΔE and I_{-2} at –2ΔE (cathodic polarization), yet another equation for corrosion current was derived by Jankowski [17] (known as Four Point Method (FPM)) and is as follows,

$$I_{corr} = \frac{I_1 I_{-1}}{\sqrt{I_2 I_{-2} - 4 I_1 I_{-1}}} \qquad \text{----------2)}$$

In the present studies, corrosion currents were calculated using only two methods under TPM as well as FPM and plotted as a function of the overpotential after normalizing with respect to the area of the specimen (Fig. 6a, b). It was observed that the corrosion rates calculated using Method1 continuously increased with overpotential and that the corrosion rates were much higher for 9Cr-1Mo without any addition. The specimens with the additions of B and B+Ce showed almost equal corrosion rates under Method1. However, the corrosion rates calculated by Method2 showed a different trend. The specimen with the addition of B showed the lowest corrosion rates as compared to the one with the addition of B+Ce; specimen without any addition showed the highest corrosion rates.

In one of the recent findings [24], the average PSD of the measured current noise PSD(I) at higher frequency interval (from 10 mHz to 250 mHz) was found to have correlated well with the corrosion current density as,

$$\overline{PSD(I)}\ (\varpi_2 - \varpi_1) = \frac{1}{(\varpi_2 - \varpi_1)} \sum_{\varpi_1}^{\varpi_2} F(\varpi)^2 \Delta\varpi$$

where $\omega_2 - \omega_1$ is the frequency interval on a log scale, $F(\omega)^2$ is the PSD value of the electrochemical current in decibels (A), and ω is the frequency step on a log scale. The corrosion current density to which electrochemical noise was correlated expressed the general or uniform corrosion rate. This correlation between PSD (I) and I_{corr} values confirmed earlier was used here to study the relative tendency of corrosion of two steels in two different environments [19]. The PSD (I) values were obtained between 10^{-2} Hz to 1Hz. The corrosion rates were also obtained as a reciprocal of the noise resistance ($1/R_N$, where R_N is given by the ratio of σ_V/σ_I) as it was established that R_N and polarisation resistance (R_p) were equivalent, ($R_N \approx R_p$) [25] and later confirmed in some laboratories [26, 27]. Corrosion rates calculated using FPM, PSD (I) and $1/R_N$ are shown in Fig. (7a, b). From the plots of PSD (I) vs. time, it is observed that the corrosion rates of the specimen without any addition were much higher compared to the other two specimens with the additions of B and B+Ce, which after an initial decrease remained invariant; the corrosion rates for the B added specimen were much less compared to the one with B+Ce addition (Fig. 6a). Corrosion rates obtained by $1/R_N$ showed an initial slight decrease in the corrosion rate which was followed by the invariant trend in the corrosion rates for the specimen without any addition. The corrosion rates for the specimen with B+Ce addition were very similar to the specimen without any addition and were found to be invariant with time. Corrosion rates of the specimen with B addition showed the lowest corrosion rates obtained by PSD (I) as well as $1/R_N$ values. The average corrosion rates obtained by Method 1, Method 2 and FPM were compared with those obtained by Tafel fit technique (Table 3). It was noted that identical average corrosion rates

were obtained for specimens with B and B+Ce additions by Method 1(TPM) and FPM; however, the specimen with the addition of B showed much lower corrosion rates compared to the one with B+Ce addition obtained by Method 2 (TPM) as well as Tafel fit technique. Corrosion rates of 9Cr-1Mo without any addition were significantly higher compared to other specimens with B and B+Ce additions in all these measurements.

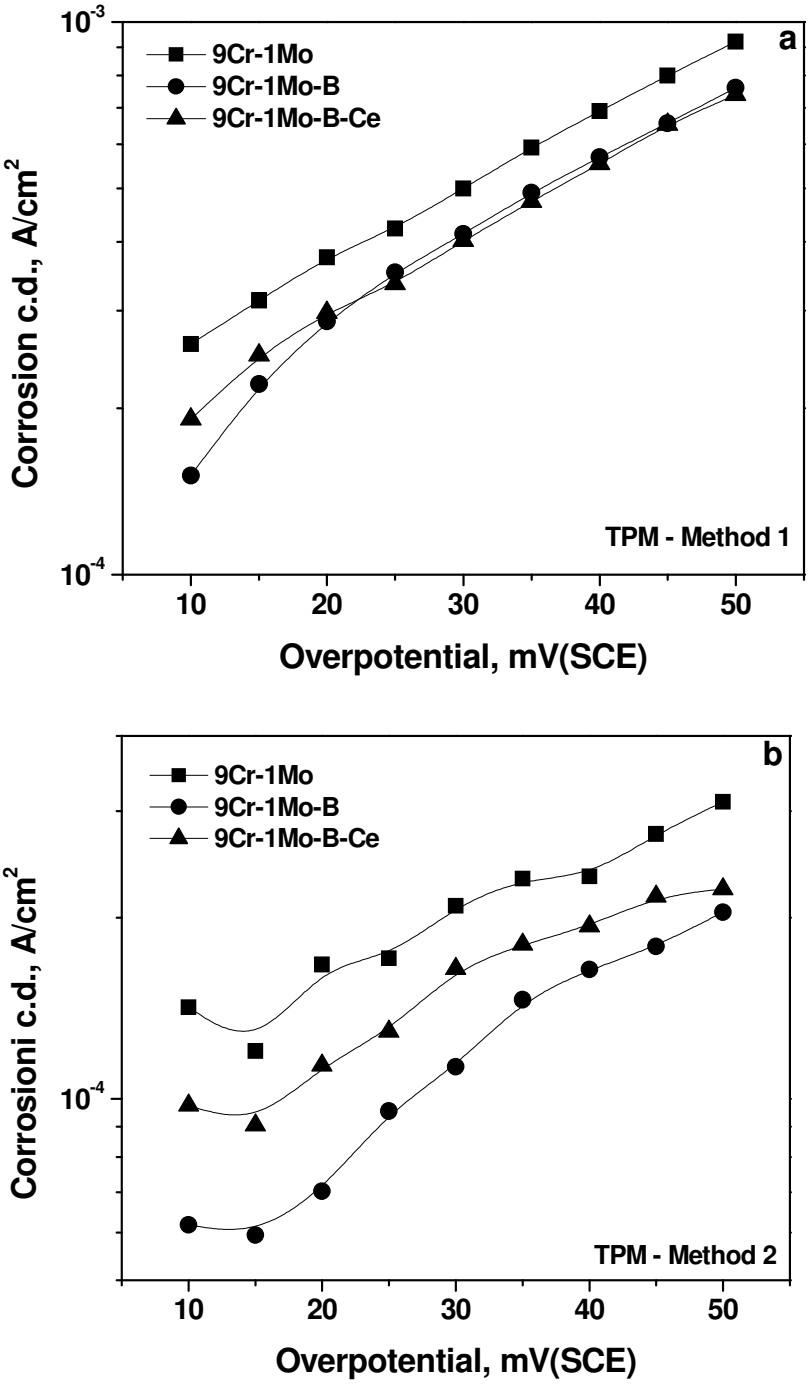

Figure 6. Corrosion rates obtained by Method 1 (a) and Method 2 (b) using TPM for 9Cr-1Mo with additions of B and B+Ce in deaerated sulphuric acid.

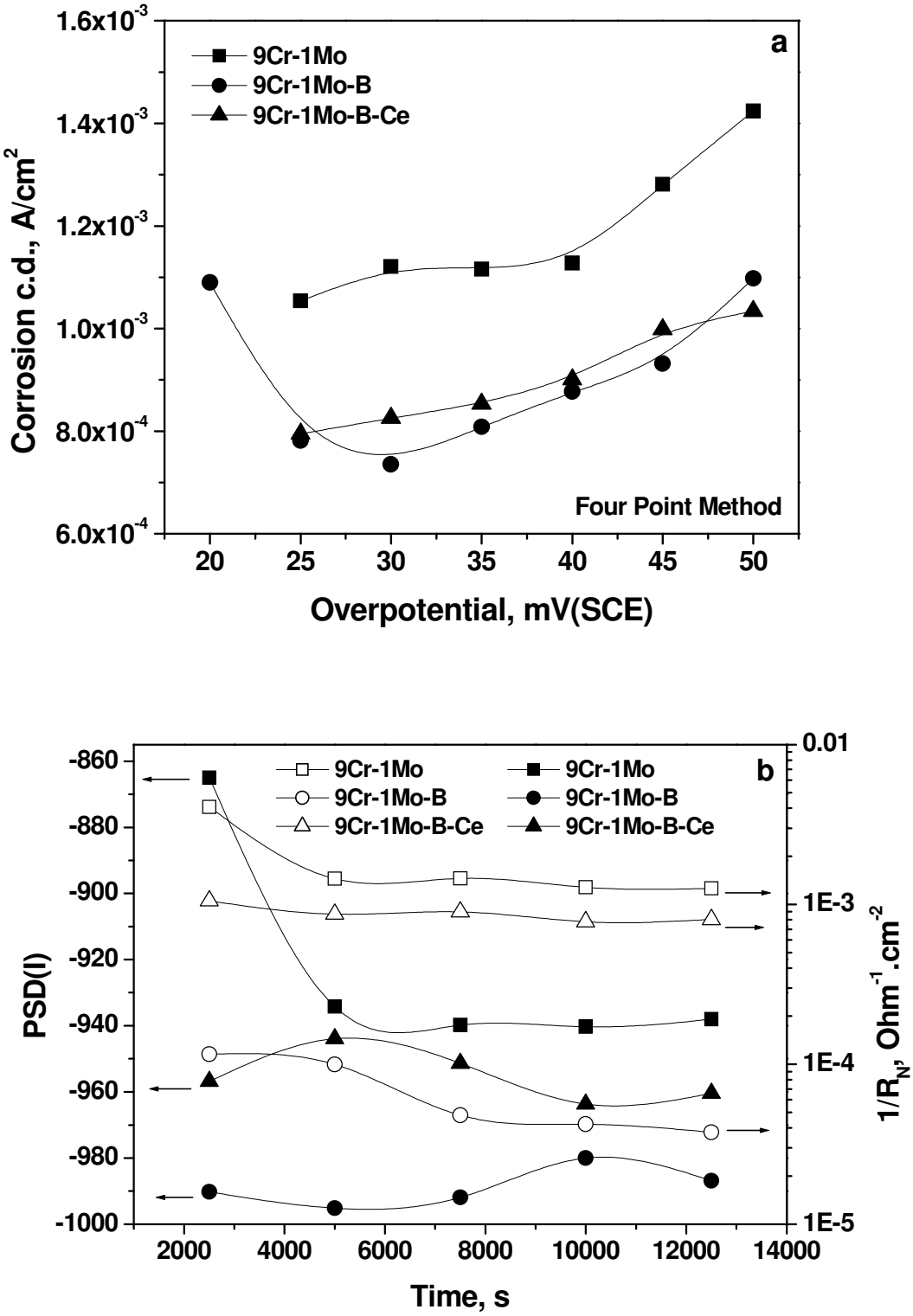

Figure 7. Corrosion rates obtained by FPM (a) and using calculated values of PSD (I) as well as $1/R_N$ (b) for 9Cr-1Mo with additions of B and B+Ce in deaerated sulphuric acid

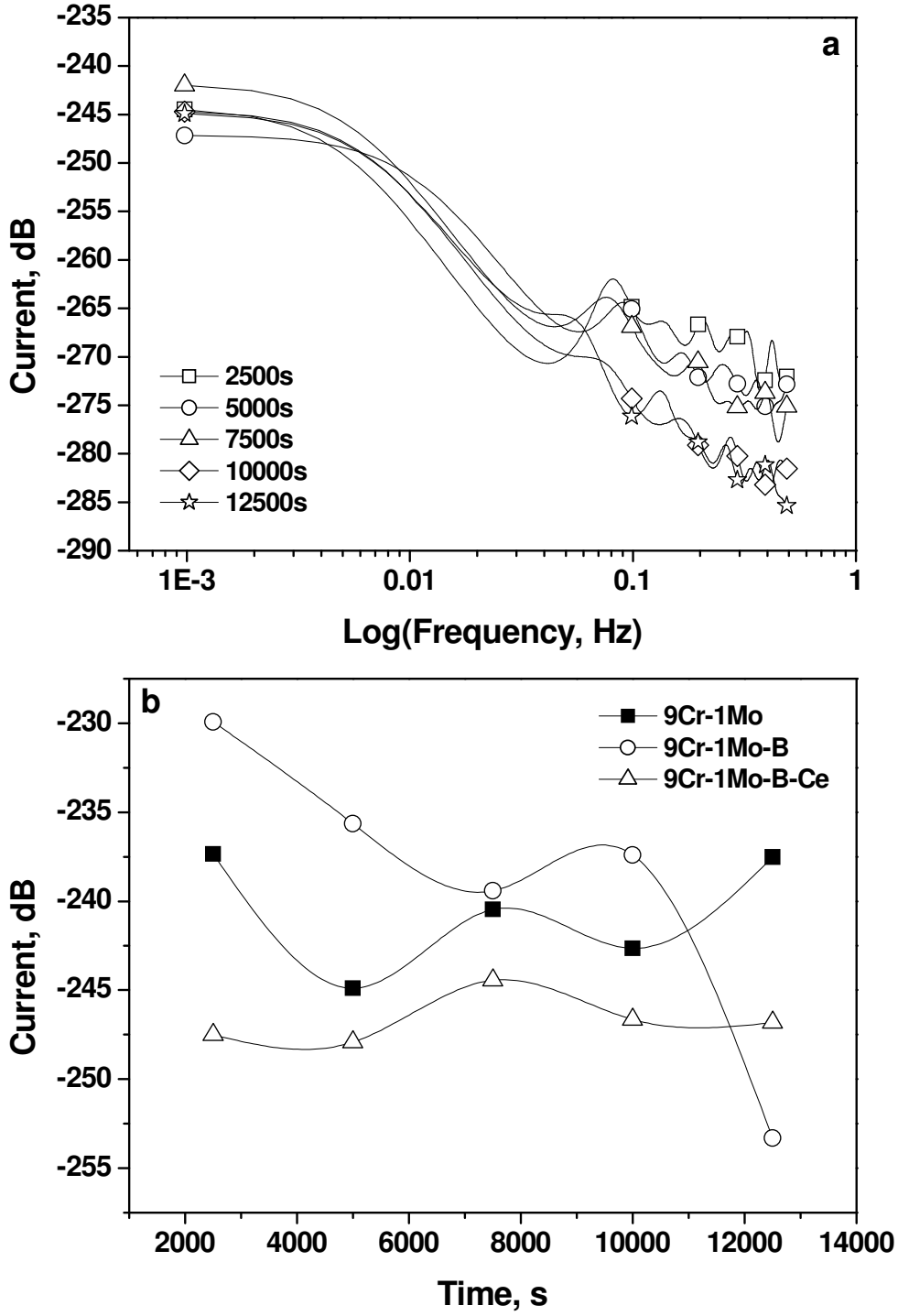

Figure 8. The current PSD plots for 9Cr-1Mo with B+Ce addition (a) and the current PSD plot in the frequency independent region as a function of time for all the specimens in deaerated sulphuric acid (b).

Earlier it was reported that the power level of the signal as calculated from the PSD in the frequency-independent region seemed to indicate the corrosion rate [28-30]. A typical current PSD

plot for 9Cr-1Mo with addition of B+Ce (Fig.8a) shows the dependence of current PSD on frequency for different time durations. It is seen that the plot can be divided into two regions, one in which the current does not vary with frequency (i.e. frequency independent region) and the other in which the current decreases continuously with frequency. The MEM allows computation of the spectra below f_{min},; however, it is imperative not to calculate PSD below f_{min} to generate misleading information [16]. Thus the PSD values calculated at f_{min} = 3.91 x 10^{-3} Hz were used to plot (Fig.8b). Although it was observed that 9Cr-1Mo with the addition of Boron initially showed the higher corrosion rate compared to 9Cr-1Mo without any addition, the corrosion rate of the former decreased with time and reached the lowest value at the end of the 12500s. The corrosion rate of the specimen with the addition of B+Ce was found to be the lower compared to the other two and that of the specimen without any addition showed a tendency to increase with time. Thus, taking into account all the results obtained so far, it was concluded that though addition of both B and B+Ce was useful in decreasing the uniform corrosion rate of 9Cr-1Mo drastically, addition of B seemed to be somewhat more beneficial compared to B+Ce on account of the better passivability offered by it.

Table 3. Comparison of the average corrosion rates obtained by TPM and FPM with those obtained by Tafel fit technique

Technique	**Average corrosion rate, A/cm^2**		
	9Cr-1Mo	**9Cr-1Mo (B)**	**9Cr-1Mo (B+Ce)**
Method1 (TPM)	6.77E-04	5.41E-04	5.41E-04
Method2 (TPM)	2.58E-04	1.52E-04	1.96E-04
FPM	1.48E-03	1.13E-03	1.13E-03
Tafel Fit	7.56E-04	5.85E-04	6.45E-04

4. CONCLUSIONS

From the results of the various investigations discussed above, the following conclusions were drawn:

1. The passive film of the B added specimen was more stable than that of the B+Ce added one. The passive film of the specimen without any addition was found to be least stable among all. This was confirmed from the current records too, which showed cathodic current signals throughout experimental duration for the B added specimen; however, specimens with and without the addition of B+Ce showed anodic current signals, indicating slow dissolution of the passive film.
2. The results of the analysis of the statistical parameters reinforced above views that B added specimen dissolved more slowly compared to other two steels in deaerated sulphuric acid.

3. Corrosion rates calculated by using TPM, FPM as well as Tafel fit technique showed that the specimen with B addition showed somewhat superior corrosion resistance compared to the specimen with B+Ce addition. The current PSD data showed marginally better corrosion resistance for the B+Ce added specimen compared to the B added specimen. However, in the long term studies, the corrosion rate of the B added specimen would be lower than that of the B+Ce added one.

Taking into account all the factors like easy passivation, stability of passive film and its dissolution and calculated corrosion rates by different techniques, it could be concluded that the specimen with B addition showed the best overall corrosion resistance compared to the B+Ce added one in deaerated sulphuric acid.

References

1. V. L. Hill and M. A. H Howes, *Mater. Performance* 17(6) (1978) 22
2. L. Henderson and R. Stead, *Nucl. Technol*. 29(2) (1976) 174
3. A. K Khare. (ed.), Ferritic Steels for High Temperature Applications, Conf. Proc. Am. Soc. For Metals, Metal Park, Ohio (1983) 210
4. G. J. Bignold, Proc. Conf. on Ferritic Steels for Fast Reactor Steam Generators, 2 (1978) 346
5. C. Willby and J. Walters**,** Proc. Conf. Ferritic Steels for Fast Reactor Steam Generators, London. 1(1978) 40
6. S.C. Tjong and M. C. Wong, *Applied Surface Science* 64(1993) 127
7. M. Naka, K. Hashimoto and T. Masumoto, *Journal of Non-Crystalline Solids*, 28(3) (1978) 403
8. T.P. Moffat, R. M. Latanision and R. R. Ruf, *J. Electrochem. Soc*. 139(4) (1992) 1013.
9. F. M. Seon, *Journal of the Less-Common Metals*, 148 (1-2) (1989) 73
10. Y. Okanda, M. Fukusumi, S. Nenno and J.B. Newkirk, *Metall. Trans*., 14A(10) (1983) 2131.
11. Y. Okanda, M. Fukusumi, K. Mizuuchi and S. Nenno, *Trans. Jpn. Inst. Met*., 27(9) (1986) 680
12. S.L. Langenbeck, J. M. Cox and R. F. Simenz, Rapidly Solidified Powder Aluminum Alloys, Am. Soc. For Testing and Materials, Philadelphia, PA, 1986, p. 450.
13. N. Valverde, *Rev. Metal*. 21(3) (1985) 143
14. N. Parvathavarthini, R.K. Dayal and J.B. Gnanamoorthy, *Bull. Electrochem*. 6(1) (1990) 20.
15. R. A. Cottis, *Corrosion* 57(3) (2001) 265
16. U. Bertocci, J. Frydman, C. Gabrieelli, F. Huet and M. *J.* Keddam, *Electrochem. Soc*. 145(8) (1998) 2780
17. M. J. Danielson, *Corrosion* 38(11) (1982) 580
18. J. Jankowski and R. Juchniewicz, *Corros. Sci.* 20(7) (1980) 841
19. M.G. Pujar, N. Parvathavarthini and R.K. Dayal, *Corrosion Prevention and Control* 51(1) (2004) 30
20. O.P. Modi, M. N. Mingole and K. P. Singh, *Corrosion Sci.* 30(8-9) (1990) 941
21. N. Parvathavarthini, R.K. Dayal and J.B. Gnanamoorthy, *Corrosion* 52(7) (1996) 540
22. C. Wagner and W. *Z.* Traud, *Elektrochem*. 44(1938) 391
23. S. Barnartt, *Electrochem. Acta* 15(8) (1970) 1313
24. A. Legat and V. Dolecek, *Corrosion* 51(4) (1995) 295
25. A. Aballe, A. Bautista, U. Bertocci and F. Huet, *Corrosion* 57(1) (2001) 35
26. F. Mansfeld and H. *J.* Xiao, Electrochem. *Soc.*140(8) (1993) 2205
27. Y. J. Tan, S. Bailey and B. Kinsella, Corros. *Sci.* 38(10) (1996) 1681
28. I. A. Al-Zanki, J. S. Gill and J. L. Dawson, *Materials Science Forum* 8(1986) 463

29. G. Gusmano, G. Montesperelli, S. Pacetti, A. Petitti and A. D'Amico, *Corrosion* 53(11) (1997) 860
30. G. Gusmano, G. Montesperelli, A. D'Amico and C. Di Natale, Use of noise measurements for the investigation of corrosion phenomena, Proceedings from Corrosion Asia 1994-The Second NACE Asian Conference held September 26 through 30, Corrosion Asia, Singapore, Houston, TX: NACE, 1994, pp 1045-1 to 1045-10